ARTICLES

An Investigation into the Initial Degradation Steps of Four Major Dye Chromophores: Study of Their One-Electron Oxidation and Reduction by EPR, ENDOR, Cyclic Voltammetry, and Theoretical Calculations

Tsvetanka Stanoeva,[†] Dmytro Neshchadin,[†] Georg Gescheidt,*[,†] Jiri Ludvik,[‡] Barbora Lajoie,[‡,§] and Stephen N. Batchelor*[,||]

Institute of Physical and Theoretical Chemistry, Graz University of Technology, Technikerstrasse 4/I, 8010 Graz, Austria, Department of Electrochemistry, J. Heyrovsky Institute of Physical Chemistry, Academy of Sciences of the Czech Republic, Dolejskova 3, 18223 Praha 8, Czech Republic, Unilever Research, Port Sunlight, Quarry Road East, Bebington, Wirral, CH63 3JW, U.K., and Laboratory of Bioinorganic and Medical Chemistry, University Paul Sabatier, 38 rue des Trente-six Ponts, 31400 Toulouse, France

Received: June 29, 2005; In Final Form: September 21, 2005

The degradation of dyes is frequently initiated by one-electron oxidation or reduction; however, relatively little is known about the initially formed radicals. Acid Green 25 (**AG25**), Crystal Violet (**CVI**), Methylene Blue (**MB**), and Acid Orange 7 (**AO7**), representing paradigms of four types of commercial organic dyes, were therefore investigated in terms of their redox behavior. Their redox potentials in MeCN and buffered aqueous solutions were determined by cyclic voltammetry. The structures of the one-electron reduced and oxidized dyes were established by EPR spectroscopy and by theoretical calculations on the density functional level of theory.

Introduction

Synthetic dyes are used to color many different products, such as textiles, paper, food, cosmetics, and drugs. They represent a substantial part of the chemical industry with an annual production of nearly one million tons.[1] Most modern dyes are designed to be highly stable chemically, to provide a consistent color in use. However, on disposal, methods to effectively destroy the dyes are required to prevent environmental damage.[2] In nature, dyes are frequently destroyed by enzymatic reactions within living organisms, which can have important implications for environmental and human safety. In many cases, the dyes are degraded via initial one-electron oxidation or reduction reactions, for example: the metabolism of many dyes in the human body is mainly due to one-electron reduction by enzymes in the liver or in intestinal anaerobic bacteria;[3] in the environment a one-electron photooxidation is a predominate degradation route,[4] and both one-electron oxidation and reduction have been investigated as means of destroying effluent with photoinduced reactions.[5−8] Consequently, mechanistic insights in the chemistry of dye destruction are desirable from a variety of quarters and interests.

Despite the importance of these one-electron reduction and oxidation reactions, relatively little is known about the properties of the initially formed radical species, which are key intermediates in final product formation. On one hand, this is rather astonishing since synthetic dyes have been used for over a hundred years;[1] on the other hand, however, it is very difficult to attain a complete and consistent set of the corresponding data and a clear-cut analysis, as will be shown below. To help fill this knowledge gap, a study of 4 dyes and their reduced and oxidized forms is reported here. Primarily the dyes are converted to their radical cations and radical anions by the oxidation or reduction step.

Therefore, the focus of the current study is the determination of the thermodynamic and kinetic stability of one-electron reduced and oxidized dyes by cyclic voltammetry. The paramagnetic ions are characterized by EPR and ENDOR spectroscopy supported by calculations on the density functional level of theory. As dyes are used in both hydrophobic and hydrophilic environments, where possible the CV were performed in acetonitrile (MeCN) and in water. MeCN provides a more ideal system where dye aggregation does not occur and in which protonation/deprotonation equilibria are suppressed, leading to intermediates of higher persistence. For this EPR and ENDOR study the dyes were reduced/oxidized by appropriate methods in organic solvents to provide reaction conditions favoring the detection of the primarily formed species.

The dyes, shown herein, were chosen to represent important chromophore classes. Anthraquinone dyes, represented by Acid Green 25, **AG25**, are widely used to dye textiles. Crystal Violet (Basic Violet 3), **CVI**, and Methylene Blue (Basic Blue 9), **MB**, are both used as biological stains and as probes in chemical investigations. Compound **CVI** and the heterocyclic molecule **MB** represent triarylmethane and azine dyes, respectively; both

* Corresponding authors. E-mail: gescheidt@ptc.tugraz.at (G.G); Stephen.Batchelor@unilever.com (S.N.B.).
[†] Graz University of Technology.
[‡] Academy of Sciences of the Czech Republic.
[§] University Paul Sabatier.
[||] Unilever Research.

10.1021/jp053536l CCC: $30.25
Published on Web 11/15/2005

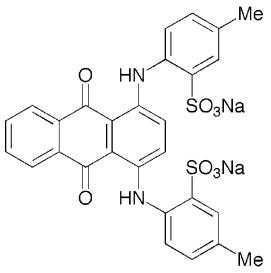

AG25

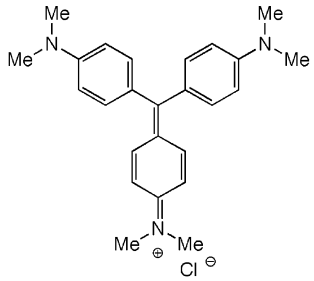

CVI

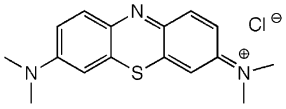

MB

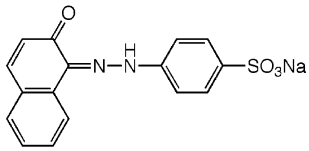

AO7

types of dyes show poor stability and are used to print and dye some synthetic textiles where permanence is not crucial. Acid Orange 7, **AO7**, is a frequently used model, for azo dyes,[9−12] which are currently utilized in a broad range of applications, e.g. textiles (most dyeing is done with azo dyes), cosmetics,[13] and food industries.[14] **AO7** is shown in the hydrazone tautomer in which it predominately exists.[15]

Experimental Section

Cyclic Voltammetry. Cyclic voltammetry measurements in nonaqueous solvents were performed on a Metrohm Polarecord E 506 and a VA scanner E 612 with a VA stand 663 (Metrohm AG, Herisau, Switzerland). All measurements were carried out in MeCN as a solvent containing 0.1 M tetra-*n*-butylammonium perchlorate as supporting electrolyte at room temperature. The working electrode was a platinum disk while platinum wire was used as counter electrode. Scan rates were 200−400 mV·s^{-1}. Ferrocene (Fc/Fc$^+$) was used as an internal reference ($E_{1/2}$ = 440 mV vs Ag/AgCl).

Cyclic voltammetry measurements in aqueous buffers were performed on a computer-controlled Eco-Tribo-Polarograph (POLARO SENSORS, Prague) using a platinum stationary disk or a hanging mercury drop as working electrodes, platinum sheet as an auxiliary electrode, and an Ag/AgCl reference electrode. The concentration of the dyes varied from 10^{-5} to 10^{-3} mol·L^{-1}. Phosphate buffers (0.1 M) were used for pH 2−3 and 5−8, acetate buffers (0.1 M) were used for pH around 4.5, and 0.05 M borate buffers were used for pH 8−10. Scan rates were 50−200 mV·s^{-1}; temperature, 20 °C.

EPR and ENDOR. For EPR measurements the samples were prepared under high vacuum. 1,2-Dimethoxyethane was refluxed over Na/K alloy and stored over Na/K alloy under high vacuum. The reduction reactions were performed by contacts of the solutions of the parent compounds with a K-metal mirror. 1,1,1,3,3,3-Hexafluoropropan-2-ol, trifluoroacetic acid, and phenyliodine(III) bis(trifluoroacetate) were purchased from Aldrich and used without further purification. Tris(4-bromophenylammoniumyl)hexachloro antimonate was synthesized according to ref 16. EPR and ENDOR spectra were recorded on a Bruker ESP 300 spectrometer. The isotropic doublet EPR spectra were simulated with Winsim,[17] a public-domain program.

Calculations. Calculations were performed with the Gaussian98 package.[18] For geometry optimization and single-point determinations of the Fermi contacts, the UB3LYP/6-31G*//UHF/3-21G* protocol was used. This procedure generally leads to a rather efficient and accurate determination of isotropic hyperfine coupling constants (hfcs).[19]

TABLE 1: One-Electron Redox Potentials of AG25−AO7 vs Ag/AgCl/mV[a]

dye	solvent	reduction E(red) (Δ)	oxidation E(ox) (Δ)
AG25	MeCN	−1020 (80)	+740 (120)
	aq buffer	−570 (150)[b]	
CVI	MeCN	−490 (100)	+1270
	aq buffer	ca. −600 (200)[b]	+850[c]
		ca. −1200[b]	
MB	MeCN	−130 (100)	+ 490 (110)
	aq buffer	ca. −650[b]	
AO7	MeCN	−990 (E_p)	+1360
	aq buffer	−560 (130)[b]	

[a] The Δ values indicate the peak-to-peak distance between quasi-reversible oxidation/reduction couples/mV; if no Δ value is given only a reduction (oxidation) peak potential is presented (E_p)) [b] 0.1 M acetate buffer pH 4.7. [c] 0.1 M phosphate buffer pH 2.8.

Results and Discussion

General Remarks. *Charges.* Generally, one-electron oxidation and reduction of a closed-shell neutral molecule leads to the formation of a radical cation and radical anion, respectively. Dyes **AG25**−**AO7** are salts of negatively (**AG25**, **AO7**) and positively (**MB**, **CVI**) charged organic molecules. Accordingly, regarding exclusively the organic moiety of these salts, one-electron oxidation of **AG25**, **CVI**, **MB**, and **AO7** leads to the formation of a radical anion, radical dication, radical dication, and neutral radical, respectively, whereas reduction leads to the radical trianion (**AG25**), neutral radicals (**MB**, **CVI**), and a radical dianion (**AO7**). Thus differently charged species are formed after identical electron-transfer reactions, which is somehow misleading. Therefore, in this paper the entire salts, i.e. the organic moiety including the corresponding counterions (Na$^+$, Cl$^-$), are regarded as the parent molecules. Consequently, one-electron oxidation gives radical cations while the one-electron reduction produces radical anions.

Cyclic Voltammetry. Measurements in MeCN led to well distinguishable cyclovoltammetric curves; however, the investigations in aqueous media were complicated by adsorption phenomena at the electrodes. The highest adsorption, which practically prevented measurements of redox potentials, was observed at the mercury electrode, where the adsorbed film blocks the surface. Even, at platinum, the shape of the curves is affected by many factors including the history of the electrode, the applied switching potentials, and temperature. The rigorous interpretation of currents is therefore challenging. Nevertheless, with an extended series of measurements at various concentrations of **AG25**−**AO7** and various scan rates, the redox behavior of these dyes can be sufficiently analyzed.

Acid Green 25 (AG25). *Cyclic Voltammetry.* In MeCN, **AG25** takes up an electron at a potential of E_p = −1020 mV vs Ag/AgCl in a partly reversible step (Table 1). This result is quite unexpected since the reduction should lead to a persistent anthraquinone-type radical anion.

The electrochemical experiments of **AG25** in protic media (acetate buffer pH 4.5) exhibit a quasi-reversible redox couple around −570 mV vs Ag/AgCl (E_{pc} = −630 mV; E_{pa} = −480 mV), which[20] we ascribe to a reversible two-electron reduction to the corresponding hydroquinone.[21] The reversibility of the reaction, i.e., the appearance of the anodic counterpeak, increases (a) with increasing concentration; (b) with increasing scan rate; (c) with increasing time of electrolysis at the switching potential

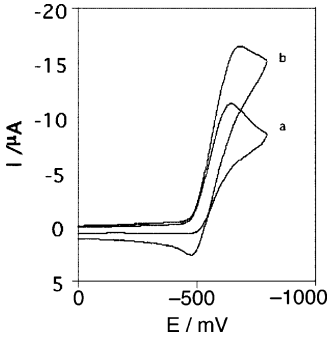

Figure 1. Cyclic voltammograms for the reduction of **AG25** (concentration 3×10^{-5} mol^{-1}) in acetate buffer pH 4.5. Scan rate 100 mV·s^{-1} (a) and 200 mV·s^{-1} (b).

during a CV experiment. This behavior points to a follow-up reaction of the reduction product, i.e., of the hydroquinone. The positive shift of the potential (with respect to the aprotic conditions) is most likely caused by fast follow-up protonation of the quinone dianion.

In borate buffer, pH 9, where the formation of the hydroquinone is attenuated (similar conditions as in MeCN), an irreversible multielectron reduction process between −800 and −1000 mV was observed, pointing to the formation of the semiquinone radical anion and semiquinone dianion at potentials compatible to those determined in MeCN.

A quasi-reversible oxidation for **AG25** at 740 mV vs Ag/AgCl is detected in MeCN, which we assign to the formation of the radical cation of **AG25**. This potential is in a range compatible with the oxidation of the 1,4-diaminobenzene moiety. In aqueous/buffered environment only an irreversible anodic oxidation at +1200 mV was observed (Figure 1). This indicates that the primarily formed diaminobenzene-type radical cations undergo deprotonation reactions in aqueous environment.

EPR Spectra. Reduction. Well-resolved EPR signals were obtained after reaction of **AG25** with Zn in DMF, which are ascribed to the corresponding radical anion of **AG25** (Figure 2). The EPR spectrum, readily simulated with hyperfine coupling constants (hfcs) of 0.005 (8 H), 0.046 (2 H), 0.158 (2 H), and 0.092 mT (2 N), mirrors an amino-substituted 9,10-anthraquinone radical anion in which the spin and the charge are confined to the central quinone moiety. These data are in agreement with those of related 2,4-diamino-substituted anthraquinone radical anions which are iso π electronic to **AG25**$^{\bullet-}$.[22] Remarkably, standard reduction procedures with Na or K metal as the reducing agents (in 1,2-dimethoxyethane or THF as the solvents) only led to very weak signals. This observation is in very good agreement with the results of the electrochemical measurements: the considerable reducing power of Na and K leads to the formation of the EPR-silent dianion.

Oxidation. Chemical oxidation of **AG25** with a number of oxidants such as tris(4-bromophenyl)ammoniumyl hexachloroantimonate,[16] trifluoroacetic acid, and phenyliodine(III) bis(trifluoroacetate) (PIFA)[23] yielded a partially resolved EPR signal (Figure 2). The dominating seven-line EPR pattern is produced by the interaction of the unpaired electron with two equivalent ^{14}N and ^{1}H nuclei with hfcs of 0.505 (2 N) and 0.577 (2 H) mT. These values are consistent with the calculated ones of 0.465 and 0.615 mT, respectively, and with values of related 1,4-diamino-substituted anthraquinones.[24] The hfcs of the remaining protons are not resolved. The spin and the charge in **AG25**$^{\bullet+}$ are concentrated within the formal phenylenediamine moiety with only a small portion being delocalized into the adjacent naphthoquinone. When the oxidation is performed in

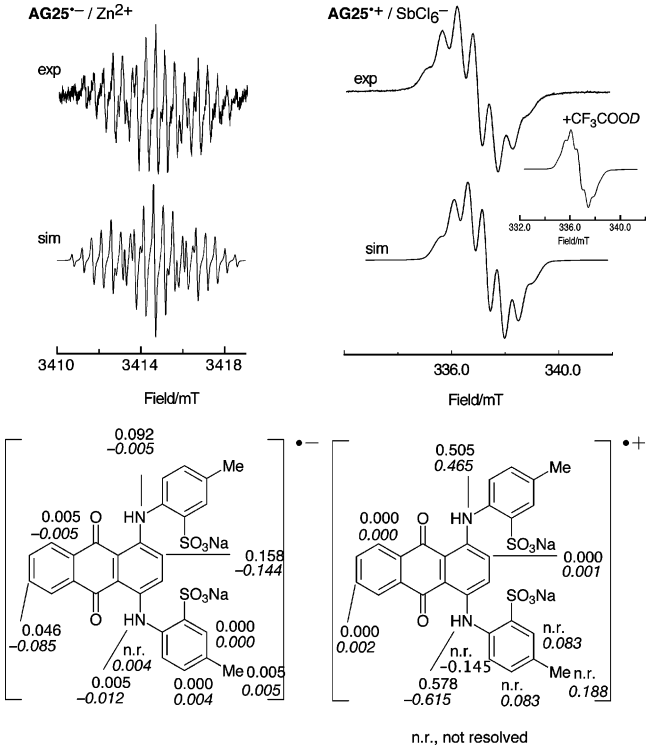

Figure 2. Experimental and simulated EPR spectra assigned to one-electron reduced (left) and oxidized (right) **AG25** together with experimental and calculated (in italics) hfcs and their assignment. The additional EPR spectrum (right) shows the signal attributed to **AG25**$^{\bullet+}$ in which the N*H* protons are replaced by deuterium.

the presence of CF_3COOD, the ^{1}H hfc of 0.577 (2 H) mT is replaced by a ^{2}H hfc of 0.067 mT (see inset in Figure 2). This exchangeable N*H* proton indicates that a hydrogen bridge C═O···H···N is formed in the radical cation. The dynamics of this H-bridge, however, do not become apparent on the hyperfine time scale of our experiment since no spectral alterations in the temperature range between 193 and 298 K were observed.

Crystal Violet (CVI). *Cyclic Voltammetry.* For **CVI**, a quasi-reversible reduction can be established at −490 mV vs Ag/AgCl in MeCN (Table 1). In acetate buffer at pH 4.5 a redox couple emerges at −600 mV vs Ag/AgCl (E_{pc} = −700 mV; E_{pa} = −500 mV). The intensity of the anodic counterpeak increases (a) with increasing concentration; (b) with increasing scan rate pointing to follow-up reactions. An increasing time of electrolysis at the switching potential during a CV experiment had no influence on the anodic peak. A second reduction process follows at −1200 mV at the edge of our detection range (partly masked by the signal due to the destruction of the electrolyte).

In MeCN, a quasi-reversible one-electron oxidation can be established at +1270 mV vs Ag/AgCl. At pH 2.8, this electron transfer proceeds irreversibly at +850 mV and the follow-up product is reduced during the reverse scan at +300 mV. The anodic oxidation under strongly acidic conditions was attributed to the formation of the quinoid *N*,*N*,*N*′,*N*′-tetramethylbenzidine dication which is reduced at +300 mV.[25]

EPR Spectra. Reduction. A well-resolved EPR spectrum emerges after reduction with K in 1,2-dimethoxyethane (DME). With the help of the ENDOR technique, a matching simulation can be achieved (Figure 3). The ENDOR spectrum reveals ^{1}H hfcs of 0.239, 0.090, and 0.081 mT, due to 6, 6, and 18 equivalent protons, respectively (according to the EPR simulation). Moreover an additional ^{14}N hfc of 0.113 mT for three equivalent nuclei has to be added. The experimental and the calculated hfcs are in close agreement. Addition of an electron

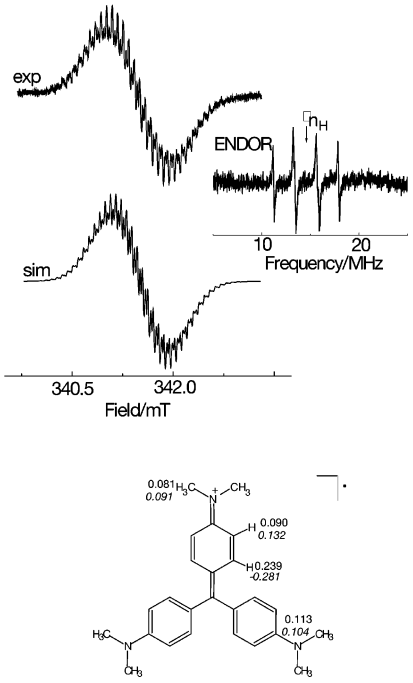

Figure 3. EPR and ENDOR spectra of **CVI**$^{\bullet-}$ (T = 213 K) together with experimental and calculated (in italics) hfcs and their assignment.

to parent **CVI** (formally carrying one positive charge) leads to the formation of a neutral 19-carbon-atom π system with 19 electrons. This species resembles a triphenylmethyl-type radical of C_{3v} symmetry on the hyperfine time scale with the spin and the charge being evenly distributed between all three phenyleneamine groups.

Oxidation of **CVI** with PIFA in HFP/TFA (10:1) leads to a well-resolved EPR spectrum. The simulation of this signal can be successfully accomplished with the hfcs provided by ENDOR. The dominating hfcs of 0.610 mT (2 ^{14}N) and 0.649 mT (12 ^{1}H) have to be ascribed to two dimethylamino groups. The smaller hfcs of 0.297 and 0.122 mT (each for 4 equiv ^{1}H) are assigned to the *ortho* and *meta* protons of the phenyl groups (Figure 4). In contrast to the radical obtained upon reduction of **CVI** these data represent the delocalization of the unpaired electron within *two N*,*N*-dimethylaminobenzene moieties. Thus, the delocalization of the unpaired electron and the additional positive charge does not extend into the positively charged quinoid moiety. This electron distribution is also predicted by theoretical calculations and leads to a very good agreement between experimental and calculated hfcs. Significantly these data do *not* correspond to those assigned to the radical cation of *N*,*N*,*N*′,*N*′-tetramethylbenzidine, the rearrangement product formed upon oxidation of **CVI** in acidic solution.[26]

Methylene Blue (MB). *Cyclic Voltammetry.* In MeCN, **MB** can be reduced at −130 mV vs Ag/AgCl in a quasi-reversible step. This relatively low reduction potential is in line with its extended π system and the favorable electron-accepting properties of the central nitrogen-containing heterocycle,[27] and agrees with work on similar dyes.[28] The electrochemical experiments of **MB** in protic media (acetate buffer pH 4.5) exhibit an irreversible reduction peak at around −650 mV vs Ag/AgCl (which is shifted to more negative values with increasing scan rate). This first reduction reaction can be explained by reduction of the cationic dye by two electrons and one proton connected with the structural change (from quinoid to reduced thiazo heterocycle. Another reduction process appears at −1100 mV (merging into the discharge current) which is partly reversible (E_{pa} = −950 mV). In borate buffer pH 9 a partly reversible

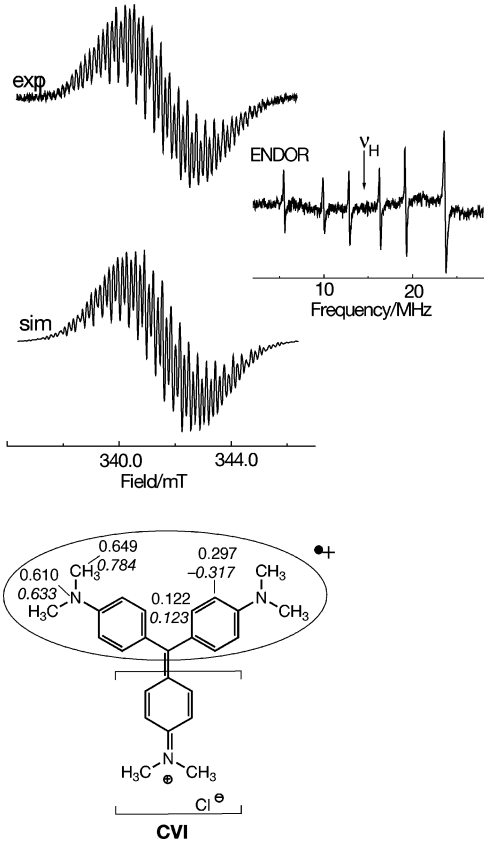

Figure 4. Experimental and simulated EPR spectra of one-electron oxidized **CVI** together with the corresponding ENDOR spectrum and the electron distribution in one-electron oxidized **CVI** together with experimental and calculated (in italics) hfcs and their assignment.

multielectron reduction process occurs between −800 and −900 mV with the anodic counterpeak at 750 mV. In MeCN, oxidation of **MB** is accomplished at + 490 mV vs Ag/AgCl. In acetate buffer, no oxidation process of **MB** was observed up to +1100 mV. It is very likely that oxidation affords rather high potentials outside the window of the CV experiment as corroborated by the observation that EPR spectra of oxidized (and protonated) **MB** can only be observed after oxidation with strongly oxidizing acids (see below).

EPR Spectra. Reduction. Reduction of **MB** with potassium in DME leads to a fairly well resolved EPR signal, which can be readily simulated, with the use of the data obtained from ENDOR spectroscopy and, for the ^{14}N hfcs, from calculations (Figure 5). The spin is delocalized within the entire π system with the highest hfc assigned to the ^{14}N nucleus in the heterocycle (Figure 5). This is in very good agreement with published data on the parent phenothiazine.[29]

Oxidation. Unexpectedly, attempts to oxidize **MB** with tris-(4-bromophenyl)ammoniumyl hexachloroantimonate and PIFA failed. The only way to obtain an oxidized form of **MB** was the reaction with concentrated acids such as sulfuric acid and CF_3SO_3H. Here, a partly resolved EPR signal is obtained, which is identical to that already reported some years ago.[30] The four-line pattern of the EPR signal is produced by the interaction of the unpaired electron with one ^{14}N nucleus and one proton (Figure 6) both having rather similar values of 0.626 and 0.712 mT, respectively. This spectrum has to be assigned to a protonated radical cation of **MB** where the hfcs attributed to the remaining protons and the two amino nitrogens are considerably smaller and not resolved.[30]

Orange II (AO7). *Cyclic Voltammetry.* Reduction of **AO7** in MeCN revealed a nonreversible step at −990 mV vs Ag/

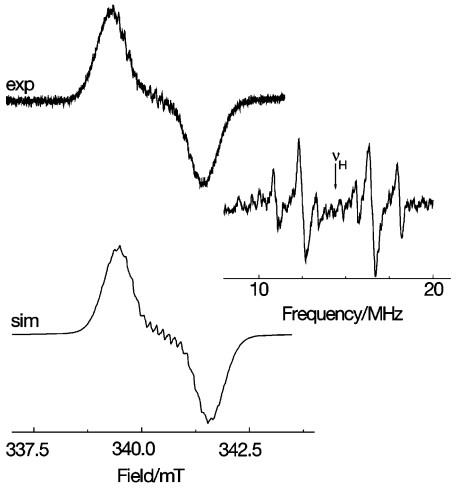

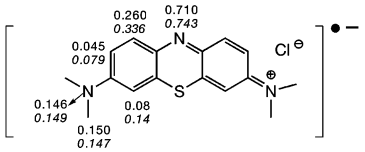

Figure 5. Experimental and simulated EPR spectra of one-electron (K/DME) reduced **MB** together with the corresponding ENDOR spectrum and the hfcs used for the simulation of the EPR spectrum together with the calculated values (in italics).

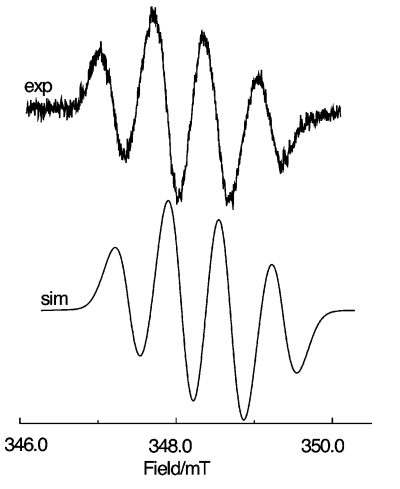

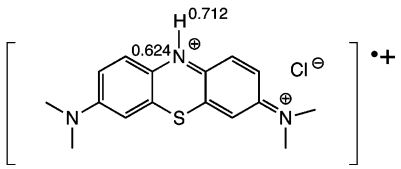

Figure 6. Experimental and simulated EPR spectra of one-electron oxidized (with H_2SO_4 at room temperature) **MB** together with its structure.

AgCl (Table 1). The electrochemical experiments of **AO7** in protic media (acetate buffer pH 4.5) exhibit a practically reversible redox couple at around −560 mV vs Ag/AgCl (E_{pc} = −620 mV; E_{pa} = −490 mV), where the reversibility depends on the starting potential: When the scan (moving toward more negative potentials) starts at +1000 mV, the reduction of **AO7** is reversible. When starting at 0 V, the reduction is irreversible. This effect is most probably connected with the anodic "cleaning" of the electrode. This is compatible with prior work,

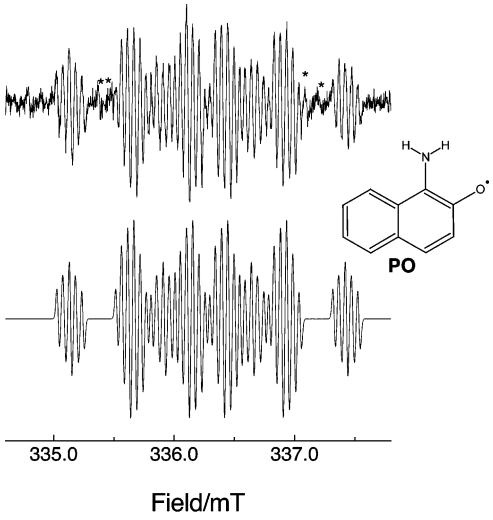

Figure 7. EPR spectrum obtained upon electrochemical reduction of **AO7** and its simulation and radical **PO** assigned to the EPR spectrum. The asterisks mark lines of an EPR signal from an additional (minor) species.

where a reversible reduction was established at −690 mV vs Ag/AgCl at pH 7 (phosphate buffer).[31] In MeCN, an irreversible signal at +1360 mV vs Ag/AgCl was detected for the oxidation of **AO7**. No anodic oxidation process at pH between 1 and 9 was observed in aqueous environment. This agrees with the results from pulse-radiolysis investigations which estimated that the corresponding oxidation potential was >1000 mV vs Ag/AgCl for an analogous dye.[32]

EPR Spectra. Reduction. Only upon electrolytic reduction of **AO7** inside the microwave cavity of the EPR spectrometer a well-resolved spectrum was obtained (Figure 7; hfcs/mT for simulation: 0.044 (1H); 0.059 (1H); 0.104 (1H); 0.535 (1H); 0.779 (1H); 0.487 (1N)). This spectrum, however, cannot be assigned to the radical anion of the parent compound, but to a rearranged product. We suggest amino phenoxy structure **PO** which has already been proposed as a decomposition product for analogous azo dyes (Figure 7).[33] This decomposition is not unexpected since in the cyclovoltammetric measurements irreversible behavior has been established revealing the low persistence of the parent radical anion even in organic solvents (on shorter time scales, however, detection of the parent radical anion of **AO7** is feasible[15,32,34]). Some additional lines in the experimental EPR signal indicate that at least one additional paramagnetic species is formed by the electron-transfer process. However since these lines are very weak and the EPR spectrum assigned to **PO** is the dominating component, the source of these additional lines cannot be analyzed. Phenoxy radicals with adjacent amino groups such as **PO** indicate a subtle structural behavior in terms of H bridging and solvent effects.[35,36] Therefore theoretical calculations of this radical do not lead to a satisfactory agreement with the experimental data.

Oxidation. Attempts to observe the primary product(s) of this oxidation by EPR using all chemical and electrochemical methods described in the Experimental Section failed. This is compatible with the high and irreversible oxidation potential of +1360 mV vs Ag/AgCl, which indicates the low thermodynamic and kinetic stability of the **AO7** radical cation. Only in rare cases, with protected aliphatic substituents, it has been possible to observe radical cations of intact azo compounds by EPR.[37−39] Photoinduced electron transfer has been shown to cause an immediate destruction of **AO7**.[12]

Further Experiments

Chemically induced dynamic nuclear polarization (CIDNP) is a NMR-derived method, which allows the detection of radicals and radical ions even with very short lifetimes. Reaction of a given molecule with an electron acceptor generally leads to the detection of products formed via the radical cations of the studied molecules whereas their reaction with electron donors covers the radical anion chemistry. We have performed several experiments with the dyes **AG25**−**AO7** using chloranil (2,3,5,6-tetrachlorobenzoquinone) and DDQ (2,3-dichloro-5,6-dicyanobenzoquinone) as electron acceptors and pyrilium salts as electron donors. Both pulsed (laser) and continuous (Hg−Xe lamp) irradiation was performed to induce electron transfer. Unfortunately none of these numerous attempts led to the detection of distinct CIDNP features. Presumably the CIDNP effects have been too weak due to a low conversion of the parent compounds and rather small hyperfine couplings of the products.

Optical spectra of all samples were taken before, during, and after the redox reactions and the EPR experiments. In all cases, the intense absorptions of the parent dyes were hardly deteriorated, i.e., no specific additional electronic spectra of the electron-transfer generated radicals could be observed in the range between 220 and 1021.5 nm. This, however, is not too astonishing since the redox reactions performed in our experiments are not quantitative and the intense absorption bands of the dyes mask those of the products.

Conclusions

The destruction of dyes, whether desired or not, frequently occurs via electron transfer.[6,40−46] Therefore the structure of the initial open-shell species has to be regarded as being crucial in understanding the mechanistic pathway of dye bleaching. Generally all representative types of molecules **AG25**−**AO7** consist of extended π systems carrying electron-donating or electron-accepting substituents which determine the color of the dye and polar groups to make them water soluble. All these dyes form π type radicals or radical ions upon the initial electron transfer. For all but **AO7**, these species are persistent in organic solvents in the absence of oxygen. In the case of **AG25** and **CVI**, the persistence of the radicals can be traced back to exceptionally persistent open-shell species such as semiquinones (**AG25**$^{\bullet-}$), Wurster's blue type radical cations (**AG25**$^{\bullet+}$), substituted trimethylphenyl radicals (**CVI**$^{\bullet-}$), or elongated phenylene diamines (**CVI**$^{\bullet+}$). Here the molecular skeletons can only be transformed into (colorless) products when additional hydrogen and electron-transfer reactions take place. For **AG25** two additional electrons and protonation lead to hydroquinones, which reveal weaker absorptions in the visible region. Alternative routes involve the reaction of molecular oxygen yielding peroxy radicals (e.g. for the formally neutral open-shell π system of **CVI**$^{\bullet-}$) causing the destruction of the molecular π system via rearrangement reactions. Moreover, **AG25**$^{\bullet-}$ and **AO7**$^{\bullet-}$ are able to act as electron donors and produce the superoxide anion, a reactive oxygen species which can be transformed to hydroxy radicals (further electron-transfer and Fenton reactions).

Upon oxidation under acidic conditions, the conjugation of the π system is attenuated in **CVI**, which again causes fading of the color. Protonation and rearrangement of the molecular skeleton are observed for **MB** and, particularly, **AO7**; nevertheless, the follow-up products consist of delocalized π systems.

Thus, on one hand, exhaustive reduction or oxidation represents a decisive step within the degradation route of dyes; on the other hand, the primarily formed products have to be further quenched by acids/bases or oxygen. These products then are potential activated reagents, which undergo additional electron-transfer steps or abstraction reactions. This subtle interplay of reaction sequences requires further step-by-step analysis.

Insights into the influence of protonation/deprotonation equilibria, which alter the electroactive parts of the dye molecules, were achieved by electrochemical studies in aqueous buffers at a broad range at pH 2.8 and 4.7. Our observations that adsorption phenomena of the dyes occur at the electrode imply surface-based electron-transfer induced pathways contributing to an efficient destruction of a dye. Moreover, the reduction potentials in water (acetate buffer) are very different from those obtained in the organic solvent MeCN. This reflects that different active molecular moieties are generated by protonation/deprotonation and reduction/oxidation in aqueous media.

Acknowledgment. We thank G. Caraman for preliminary measurements of redox potentials. J.L. is grateful for support of GA AVCR − A-4040304.

References and Notes

(1) Hunger, K. *Industrial Dyes: Chemistry, Properties and Applications*; Wiley-VCH: Heidelberg, 2003.

(2) Laursen, S. E.; Hansen, J.; Andersen, T. A.; Knudsen, H. H. "Danish EPA Working Report no. 10", 2002.

(3) Brown, M. A.; Devito, S. C. *Crit. Rev. Environ. Sci. Technol.* **1993**, *23*, 249.

(4) Batchelor, S. N.; Carr, D.; Coleman, C. E.; Fairclough, L.; Jarvis, A. *Dyes Pigm.* **2003**, *59*, 269.

(5) Yue, P. L.; Feng, J. Y.; Hu, X. *Water Sci. Technol.* **2004**, *49*, 85.

(6) Mu, Y.; Yu, H.-Q.; Zheng, J.-C.; Zhang, S.-J. *J. Photochem. Photobiol., A* **2004**, *163*, 311.

(7) Halmann, M., M. *Photodegradation of Water Pollutants*; CRC Press: Boca Raton, 1996.

(8) Eckenfelder, W. W. *Industrial Pollution Control*; McGrawHill: Boston, 2000.

(9) Stylidi, M.; Kondarides, D. I.; Verykios, X. E. *Appl. Catal., B* **2004**, *47*, 189.

(10) Mendez-Paz, D.; Omil, F.; Lema, J. M. *Water Sci. Technol.* **2003**, *48*, 133.

(11) Park, H.; Choi, W. *J. Photochem. Photobiol., A* **2003**, *159*, 241.

(12) Batchelor, S. N. *New J. Chem.* **2004**, *28*, 1200.

(13) *CTFA International Color Handbook*, 3rd ed.; Rosholt, A. P., Ed.; CTFA: New York, 2003.

(14) Belitz, H. D.; Grosch, W. *Food Chemistry*, 2nd ed.; Springer-Verlag: Berlin, 1999.

(15) Abbott, L. C.; Batchelor, S. N.; Oakes, J.; Lindsay-Smith, J. R.; Moore, J. N. *J. Phys. Chem. A* **2005**, *109*, 2894.

(16) Bell, F. A.; Ledwith, A.; Sherrington, D. C. *J. Chem. Soc. C* **1969**, 2719.

(17) Duling, D. R. *PEST Winsim*; NIEHS: Research Triangle Park, NC, 1995.

(18) Frisch, M. J.; Trucks, G. W.; Schlegel, H. B.; Scuseria, G. E.; Robb, M. A.; Cheeseman, J. R.; Zakrzewski, V. G.; J. A. Montgomery, J.; Stratmann, R. E.; Burant, J. C.; Dapprich, S.; J. M. Millam; Daniels, A. D.; Kudin, K. N.; Strain, M. C.; Farkas, O.; Tomasi, J.; Barone, V.; Cossi, M.; Cammi, R.; Mennucci, B.; Pomelli, C.; Adamo, C.; Clifford, S.; Ochterski, J.; Petersson, G. A.; Ayala, P. Y.; Q. Cui; Morokuma, K.; Malick, D. K.; Rabuck, A. D.; Raghavachari, K.; Foresman, J. B.; Cioslowski, J.; Ortiz, J. V.; Stefanov, B. B.; Liu, G.; Liashenko, A.; Piskorz, P.; Komaromi, I.; Gomperts, R.; Martin, R. L.; Fox, D. J.; Keith, T.; Al-Laham, M. A.; Peng, C. Y.; Nanayakkara, A.; Gonzalez, C.; Challacombe, M.; Gill, P. M. W.; Johnson, B.; Chen, W.; Wong, M. W.; Andres, J. L.; Gonzalez, C.; Head-Gordon, M.; Replogle, E. S.; Pople, J. A. *Gaussian 98*; Gaussian, Inc.: Pittsburgh, PA, 1998.

(19) Batra, R.; Giese, B.; Spichty, M.; Gescheidt, G.; Houk, K. N. *J. Phys. Chem.* **1996**, *100*, 18371.

(20) Baizer, M. M.; Feoktistov, L. C. α,α-Unsaturated Carbonyls. In *Organic Electrochemistry*; Baizer, M. M., Lund, H., Eds.; Marcel Dekker: New York, 1983; p 369.

(21) Okubayshi, S.; Yamazaki, A.; Koide, Y.; Shosenji, H. *J. Soc. Dyers Colour* **1999**, *115*, 312.

(22) Vatanen, V.; Eloranta, J. M.; Vuolle, M. *Magn. Reson. Chem.* **1999**, *37*, 774.

(23) Rathore, R.; Kochi, J. K. *Adv. Phys. Org. Chem.* **2000**, *35*, 193.

(24) Vatanen, V.; Eloranta, J. M.; Vuolle, M. *J. Chem. Soc., Perkin Trans. 2* **1998**, 2483.
(25) Galus, Z.; Adams, R. N. *J. Am. Chem. Soc.* **1964**, *86*, 1666.
(26) Smejtek, P.; Honzl, J.; Metalova, V. *Collect. Czech. Chem. Commun.* **1965**, *30*, 3875.
(27) Zhan, R.; Song, S.; Liu, Y.; Dong, S. *J. Chem. Soc., Faraday Trans.* **1990**, *86*, 3125.
(28) Guha, S. N.; Mittal, J. P. *J. Chem. Soc., Faraday Trans.* **1997**, *93*, 3647.
(29) Gilbert, B. C.; Hanson, P.; Norman, R. O. C.; Sutcliffe, B. T. *Chem. Commun.* **1966**, 161.
(30) Heineken, F. W.; Bruin, F. *J. Chem. Phys.* **1962**, *37*, 7.
(31) Bragger, J. L.; Lloyd, A. W.; Soozandehfar, S. H.; Bloomfield, S. F.; Marriotta, C.; Martin, G. P. *Int. J. Pharm.* **1997**, *157*, 61.
(32) Sharma, K. K.; O'Neill, P.; Oakes, J.; Batchelor, S. N.; Rao, B. S. M. *J. Phys. Chem. A* **2003**, *107*, 7619.
(33) Heikoop, G.; Van Beek, H. C. A. *Recl. Trav. Chim. Pays-Bas* **1977**, *96*, 83.
(34) Yadav, P.; Rao, B.; S. M.; Batchelor, S. N.; O'Neill, P. *J. Phys. Chem. A* **2005**, *109*, 2039.
(35) Thomas, F.; Jarjayes, O.; Jamet, H.; Hamman, S.; Saint, A.; Duboc, C.; Pierre, J.-L. *Angew. Chem., Int. Ed.* **2004**, *43*, 594.
(36) Scheffler, K.; Stegmann, H. B. *Z. Phys. Chem.* **1965**, *44*, 353.
(37) Gerson, F.; Sahin, C. *J. Chem. Soc., Perkin Trans. 2* **1997**, 1127.
(38) Gescheidt, G.; Lamprecht, A.; Heinze, J.; Schuler, B.; Schmittel, M.; Kiau, S.; Ruechardt, C. *Helv. Chim. Acta* **1992**, *75*, 1607.
(39) Mendicino, M. E.; Blackstock, S. C. *J. Am. Chem. Soc.* **1991**, *113*, 713.
(40) Wang, A.; Qu, J.; Liu, H.; Ge, J. *Chemosphere* **2004**, *55*, 1189.
(41) Carneiro, P. A.; Osugi, M. E.; Sene, J. J.; Anderson, M. A.; Boldrin Zanoni, M. V. *Electrochim. Acta* **2004**, *49*, 3807.
(42) Tang, J.; Zou, Z.; Yin, J.; Ye, J. *Chem. Phys. Lett.* **2003**, *382*, 175.
(43) Oezen, A. S.; Aviyente, V.; Klein, R. A. *J. Phys. Chem. A* **2003**, *107*, 4898.
(44) Tao, X.; Ma, W.; Zhang, T.; Zhao, J. *Chem. Eur. J.* **2002**, *8*, 1321.
(45) Chen, F.; Ma, W.; He, J.; Zhao, J. *J. Phys. Chem. A* **2002**, *106*, 9485.
(46) Joseph, J. M.; Destaillats, H.; Hung, H.-M.; Hoffmann, M. R. *J. Phys. Chem. A* **2000**, *104*, 301.